Vol. 86 No. 6 pp. 1539–1546 ACTA GEOLOGICA SINICA (English Edition) Dec. 2012

The depositional Environment at Shuidonggou Locality 2 in Northwest China at ~72–18 kaBP

LIU Decheng[1], GAO Xing[1, *], LIU Enfa[2], PEI Shuwen[1], CHEN Fuyou[1] and ZHANG Shuqin[3]

1 *Institute of Vertebrate Paleontology and Paleoanthtopology, the Laboratory of Human Evolution, Chinese Academy of Sciences, Beijing 100044, China*

2 *The Fourth Geological Exploration Institute of Henan Geology and Mineral Bureau, Zhengzhou, Henan 450001, China*

3 *Research Center of Paleontology & Stratigraphy, Jilin University, Changchun, Jilin 130026, China.*

Abstract: Shuidonggou site has abundant Paleolithic remains of Late Pleistocene deposition. Studying the evolution of depositional environments is essential to the comprehensive understanding of the living conditions of ancient populations. To reconstruct the depositional environment at Shuidonggou, we carried out archaeological excavations and collected systematic deposition samples at the key position of Shuidonggou Locality 2 for grain size analysis and sporopollen statistics. The environmental evolution around the Shuidonggou site generally underwent four stages at ~72–18 kaBP. During the first stage (~72–41 kaBP), the river developed with gravel and sand stratums. During the second stage (41~34 kaBP), a swamp with numerous aquatic plants formed. In the third stage (34–29 kaBP), site formation was characterized by shallow lake depositional conditions; the climate was relatively warm and humid. The marginal bank depositional conditions deteriorated during the fourth stage (29–18 kaBP), and the site underwent several dry events; the climate also became drier and colder.

Key words: Shuidonggou site, depositional environment, grain size, sporopollen, Upper Paleolithic

1 Introduction

Shuidonggou (SDG) site is a well-known Upper Paleolithic site in Northwest China. Since its discovery in 1923, many scholars from China and overseas have studied its stoneware and ancient human culture. Numerous efforts have been devoted to this region, and many scientific papers regarding its evolution have been published. The depositional environment of the Later Pleistocene strata, in which bedded Upper Paleolithic deposits remains, was also paid considerable attention. However, many researchers continue to debate on issues related to the depositional environment of Shuidonggou site. Initially, Teilhard de Chardin took it as a Quaternary loess unit (Licent et al., 1925). Some researchers held the same opinion (Zhou and Hu, 1988; Sun and Zhao, 1991), considering it a loess like sandy soil in the excavation report of Shuidonggou site in 1980 (Institute of Archeology of Ningxia Hui Autonomous Region, 2003). Gao Xing stated that its upper part resembles a floodplain alluvium with loess features (Gao et al., 2008). After his survey of the areas, Liu Decheng held that it should be classified as a lake-like deposition (Liu et al., 2009).

To further investigate the depositional environment of Shuidonggou site, we conducted a landform and Quaternary geological survey in this area through archaeological excavations from 2004 to 2007. Samples were collected at Shuidonggou Locality 2 (SDG2) for dating, grain size analysis, and sporopollen statistics. On the basis of the information on rock characteristics, sedimentary structure, grain carry features, as well as paleobotany, we reconstructed the depositional environment of Shuidonggou site at ~72–18 thousand years. This study is anticipated to add to our understanding of human living conditions during this era. The results should be of significance to the relationship between human activities and the environment.

* Corresponding author. E-mail: gaoxing@ivpp.ac.cn

2 Study Area

Shuidonggou site (38°17′N, 106°30′E, 1200 MASL) is located 18 km west of the Yellow River, on the eastern edge of Yinchuan Basin. Low hills (1400 m MASL) extend from the northeast to the southwest in its western side, and the Mu Us Desert is found in its eastern side. Biangou River drains the majority of the area, flows through SDG site from the south to the north, and finally into the Yellow River (Fig. 1).

Six terraces are found in this region. Terrace 2 (T2) is the most widely distributed, 15 m above the riverbed. It is characterized by an obvious dual structure, with gravel in the lower region and sand or silt accumulation in the upper region. Bedrock is exposed at the bottom. T2 is classified as a pedestal terrace. T1 is distributed only along the partial border of Biangou River, which also has a dual structure. Gravel is poorly sorted, and multi-band lacustrine peat accumulations lie in the upper region. T1, characterized as a superposed terrace, downcut T2 and was embedded in it (Fig. 2).

3 Profile Descriptions

SDG2 is located in the middle-lower reaches of Biangou River (38°17′51.8″N, 106°30′09.6″E). It belongs to T2 deposition. Its profile can be divided into 18 substrata, totaling 12.5 m in thickness. Detailed records of its profile may be found in the reference (Liu et al., 2009). Substrata are described as the following:

(1) Grayish yellow silt, modern surficial loose silt. 0.2 m;

(2) Brownish yellow silt, blocky structure. 0.96 m;

(3) Grayish white silt, blocky structure, firm, horizontal bedding. Contains clay or calcium-rich aggregates, less than 5 cm in size, band in shape in some places, no regular pattern in distribution, with a few redoximorphic mottles and granular charcoals between 2.7–3.5 m. 2.34 m;

(4) Light yellow silt, blocky structure, firm, horizontal bedding. Contains stone artifacts, animal fossils and ashes, Upper Paleolithic, first cultural layer of SDG2. 0.14 m;

(5) Light yellow silt, blocky structure, horizontal bedding, some grayish white calcareous silt-clay aggregates, with the diameter of 5 cm. 1.12 m;

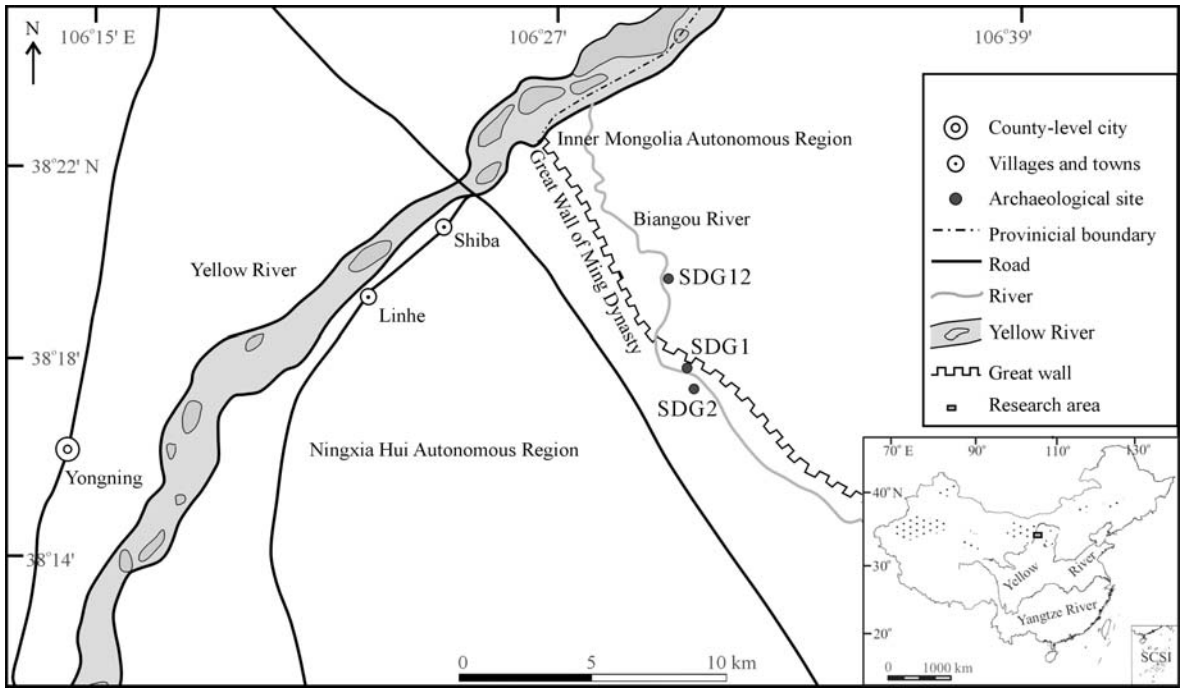

Fig. 1. Geographic position of Shuidonggou site.

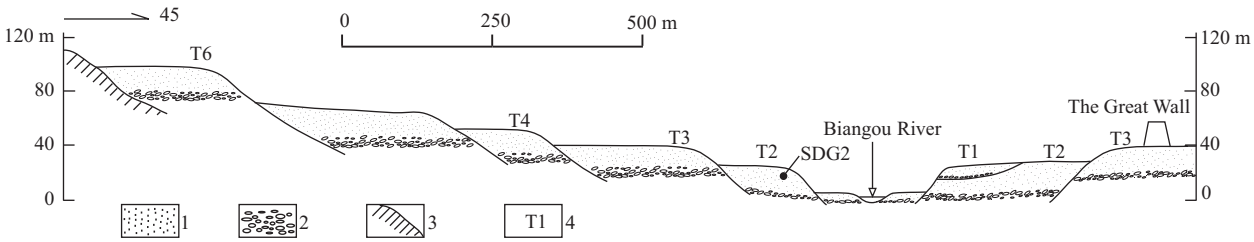

Fig. 2. The sketch of Quaternary geomorphy in the Shuidonggou region.
1, slit ; 2, gravel; 3, bedrock ; 4, terrace and serial number.

(6) Light yellow silt, blocky structure, horizontal bedding. Contains stone artifacts, animal fossils and ash, Upper Paleolithic, second cultural layer of SDG2. 0.44 m;

(7) Grayish yellow silt, compact block, horizontal bedding with a few redoximorphic mottles. 0.56 m;

(8) Light yellow silt, blocky structure, horizontal bedding. Contains stonewares, animal fossils and ash, Upper Paleolithic, third cultural layer of SDG2. 0.1 m;

(9) Light Grayish yellow silt, blocky structure, horizontal bedding with a few redoximorphic mottles. 0.44 m;

(10) Light yellow silt, blocky structure, horizontal bedding. Contains chipped stone tools, animal fossils and ash, Upper Paleolithic, fourth cultural layer of SDG2. 0.1 m;

(11) Light Grayish yellow silt, blocky structure, horizontal bedding with a lot of redoximorphic mottles, some calcareous aggregates. 0.5 m;

(12) Grayish yellow silt, blocky structure, horizontal bedding with a lot of redoximorphic mottles. 0.5 m;

(13) Light yellow silt, blocky structure, horizontal bedding. Contains stone artifacts, animal fossils and ash, Upper Paleolithic, fifth cultural layer of SDG2. 0.3 m;

(14) Light Grayish yellow silt, blocky structure, horizontal and current bedding with a lot of redoximorphic mottles, some calcareous aggregates. 0.6 m;

(15) Grayish green silt, blocky structure, horizontal and current bedding with a lot of redoximorphic mottles, some calcareous aggregates. 2.2 m;

(16) Grayish black peat, blocky, rumpled. Wormhole developed. A lot of plant remnants and small amount of gastropod, a few stone artifacts and animal fossils. 0.9 m;

(17) Grayish yellow silt and very fine sand, horizontal bedding, coarsening downward. Irregular upper and lower boundaries. 0.4 m;

(18) Gravel layer, mainly limestone, quartzite. Poorly sorted, poor rounded. Iron stains at the gravel surface. Can find reddish clay. Not to bottom. 0.7 m.

Layers 1–2 are made up of loose depositions, which are disturbed by current human activities. In our discussion and division, we focus on Layers 3 to 18. The deposition can be divided into four parts depending on lithology and sedimentary structure. Part 1 (Layers 18 to 17) contains gravel in the lower part; the gravel was aligned by flowing water. The upper part is composed of coarse to fine sand with oblique or cross bedding. The composition of Part 2 (Layer 16) changed to grayish black silt with a block structure and rumpled layer, in which wormholes developed. Numerous plant remnants and some gastropods are found. Part 3 (Layers 15–14) presents grayish green silt with horizontal and current bedding. Part 4 (Layers 13–3) presents grayish yellow silt with uniform and current bedding. Five cultural layers are found in part 4.

Several accelerator mass spectrometry (AMS) C^{14} dating taken from cultural layers are from 24 to 29 kaBP (Madsen et al. 2001; Gao Xing et al. 2003). Further dating studies devoted to the layer 17 to 4 of the SDG2 profile have been conducted recently, which yields the age range of 72.0±4.9~20.3±1.0 kaBP (Liu Decheng et al. 2009). Using optically stimulated luminescence (OSL), we determined dating at 18.0±0.9 kaBP at the middle of Layer 3. The ages of Layers 17–3 span approximately 72–18 kaBP, suggesting that it is late Pleistocene deposits. More detailed dating information can be seen from Fig. 3.

4 Experimental Analyses

4.1 Grain size analysis

Continuous samples (93) of 10 cm length were collected from the SDG2 profile, except for Layer 18. This experiment was completed by Doctor Liu Decheng of the Laboratory for Earth Surface Processes at Peking University. First, every sample was infused with 10 ml H_2O_2 at a concentration of 10% to decompose organic

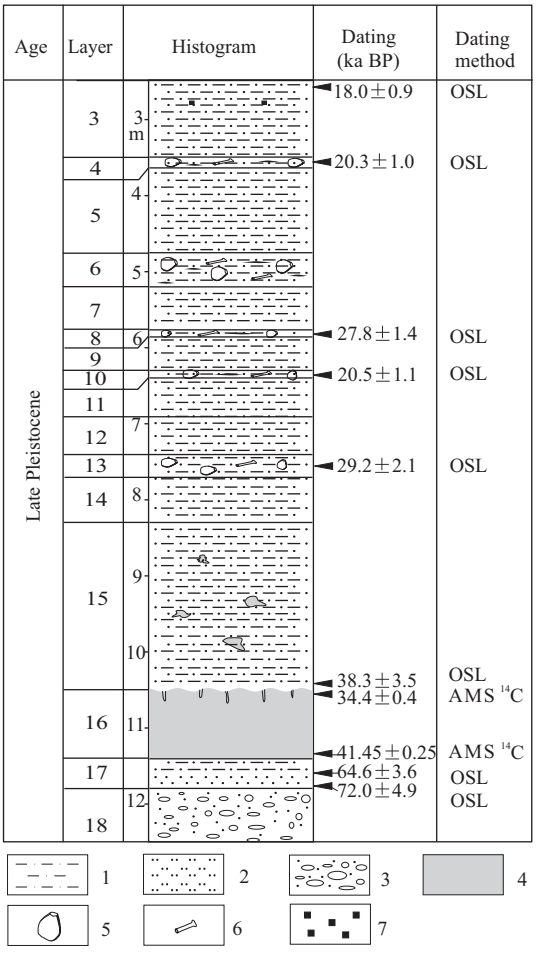

Fig. 3. Columnar section of the SDG2 profile.
1, slit; 2, fine sand; 3, sandy gravel; 4, mudstone; 5, stone artifact; 6, animal fossil; 7, charcoal. Note: Age data of AMS C14 were rectified by Intcal09.

substances. Then, superfluous HCl at a concentration of 10% was used to dissolve calcareous minerals. Second, the samples were washed until neutral, and added in $NaPO_3$ at a concentration of 5‰. Third, the samples were boiled for about 5 min and allowed to cool to room temperature. Finally, the samples were tested three times on a British-made MasterSizer2000 semi-automatic laser measuring instrument. We obtain the data for averaging. The results show that sediments were composed by silt (2–63 μm) and very fine sand (63–125 μm), accounting for 94.6% in total. Fine–coarse sand (125–2000 μm) content was low, accounting for 2.4%. The average size was 29 μm and median diameter was 58 μm. The sorting coefficient was 1.3, a value that is poor. Skewness ranged from 0.25 to 0.39, considered positive skewing, concentrated in the coarse grain terminal; this indicates that coarse grains were poorly sorted. The kurtosis value was about 1.5, considered a narrow peak.

The cumulative frequency probability of grain size and frequency curves can be divided into two combinational styles (designated as A and B). Style A consists of four aggregations, one traction aggregation, two bound aggregations, and a suspension aggregation (Fig. 4). Traction and bound aggregations intercept points dropped at 700–350 μm. The intercept point of the two bound aggregations was located at 170 μm. Therefore, this style should be characterized as a marginal bank depositional environment with less than 5% traction aggregation, up to 70% bound aggregations, and no more than 30% suspension aggregation. Its frequency curve exhibited a small apex in the coarse grain terminal, corresponding to traction aggregation. Style B consists of three aggregations, two bound aggregations, and a suspension aggregation. The traction aggregation was missing, and the frequency curve exhibited no small apex in the coarse grain terminal. The bound aggregation interval was 250–30 μm. The intercept point of the two bound aggregations swung around 100 μm. The well-sorted bound aggregation had an 80% content and a high slope rate. Style B should be characterized as lake depositional environment.

The deposition profile can be divided into two stages on the basis of grain size, sorting coefficient, skewness, and kurtosis, as well as the probability of grain size cumulative frequency curves (Fig. 4). For Stage I (Layers 17–14), the depositional carry model depicts a combination of marginal bank (represented by the black strip in Fig. 5) and lake (denoted by the white strip with a black frame in Fig. 5). Depositional average size, sorting coefficient, skewness and kurtosis fluctuated considerably, indicating high energy but unstable fluid. For Stage II (Layers 13–3), the depositional carry model is primarily lake. Grain average size, sorting coefficient, and kurtosis presented periodical fluctuation, which reflects a cyclical depositional environment, characterized by low-energy liquid conditions at a stable depositional environment as a whole.

4.2 Sporopollen analysis

To comprehensively elucidate the depositional environment in this area, we selected 27 sporopollen samples from the above-mentioned 93 samples, and sent them to the Research Center of Paleontology and Stratigraphy of Jilin University. Standard extraction

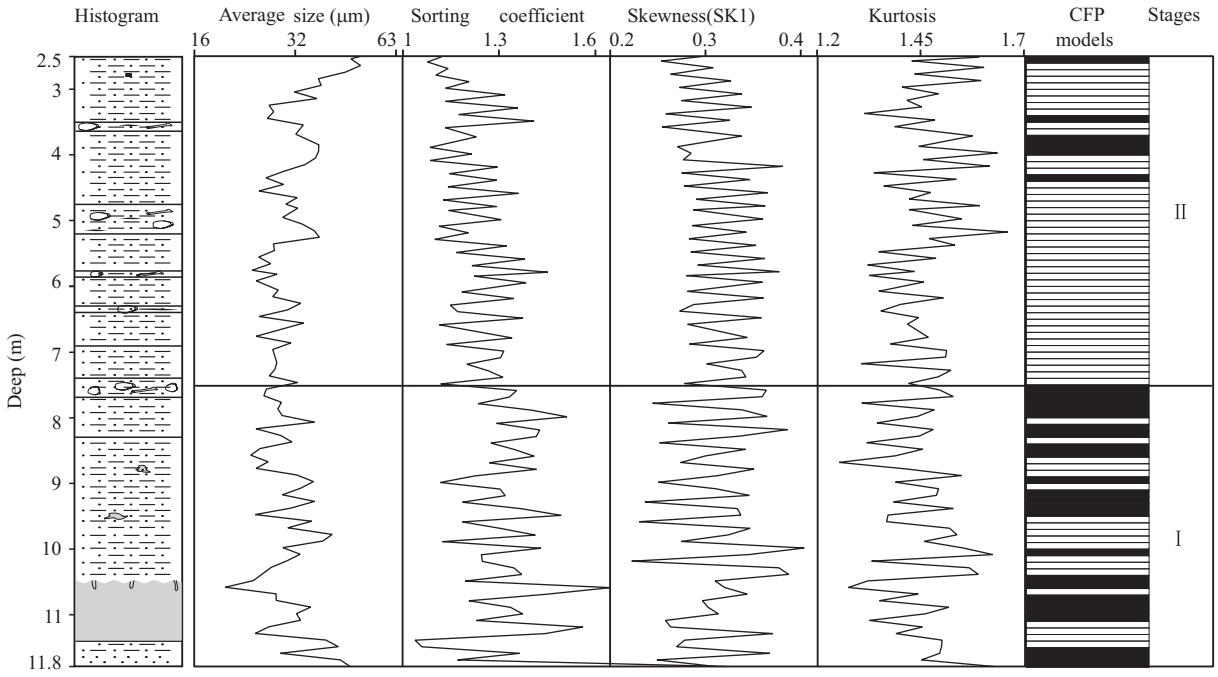

Fig. 4. Grain size cumulative frequency probability curves of SDG2.

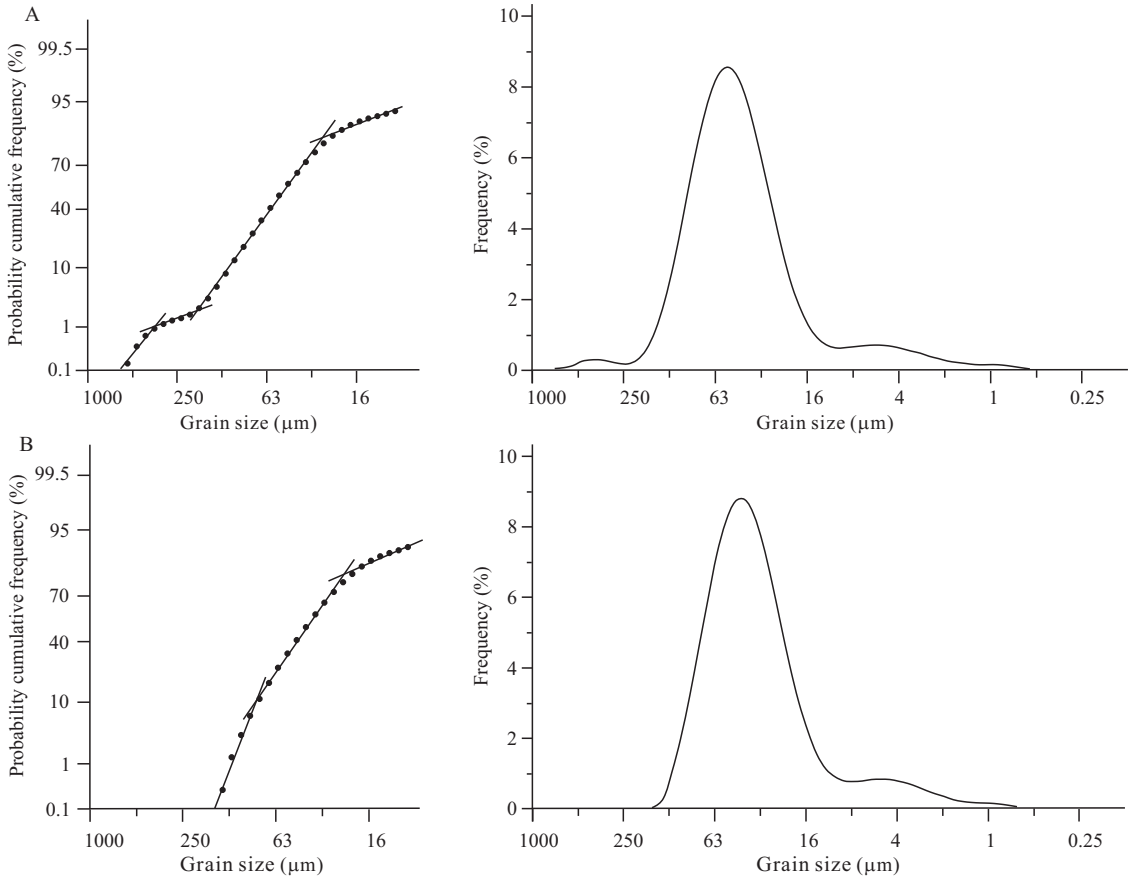

Fig. 5. Grain size parameters of the SDG2 deposition.

techniques were applied as follows: a 50 g samples were used, and 6000 brains of *Lycopodium* spores were added in every sample. The samples were then deposited by HCl→HF→HCl, and sporopollen was concentrated by Zn+HI+KI. Sporopollen was identified under a microscope. Five samples contained rich sporopollen, and 300 grains were counted for every sample. One sample was counted for 200 grains. The other 21 samples contained less sporopollen, and 100 grains were counted. A total of 3800 sporopollen grains were recognized; these belong to 55 families and genera. According to sporopollen assemblages, Sporopollen percentage curves can be divided into two strips (Fig. 6).

Strip I (Layers 17–14) was composed of 10 samples. Sporopollen concentration was high (72000 grains/g maximum, 46 grains/g minimum, 11979 grains/g on average). Fluctuation was very extensive. Herbage vegetables were prosperous, dominated at 95.9% in statistical mass. These included mainly Chenopodiaceae (22.3%), Compositae (20.9%), Cyperaceae (11.0%), *Artemisia* (10.2%), *Zygophyllum* (9.5%), and Ranunculaceae (7.4%), as well as a minimal proliferation of Saxifragaceae (4.5%) and Gramineae (2.6%). Woody pollen content was very low (3.0%), just a few *Pinus* (0.9%) and *Nitraria* (0.4%) species, etc. Strip I is categorized as a temperate grassland zone, mainly with Compositae and Chenopodiaceae, as well as a small amount of shrubs.

Strip II (Layers 13–3) was composed of 17 samples. Sporopollen concentration was extremely low (48 grains/g maximum, 7 grains/g minimum, 20 grains/g on average). A slight decrease in the proportion of herb pollen (64.2%) was observed. On the other hand, pollen from trees and shrubs increased to 26.3%, and the proportion of fern spores increased (9.5%). Terrestrial herb pollens were mainly composed of Compositae (12.8%), Chenopodiaceae (10.6%), and *Artemisia* (7.0%), as well as a small amount of Ranunculaceae (6.0%), *Zygophyllum* (5.1%), and Gramineae (4.4%). The contents of hydrophyte and wetland plants such as Cyperaceae decreased sharply from 11.0% to 1.7%. Conversely, the contents of *Typha, Lemna, Triglochin,* and *Acorus* increased to 7.4% in total. *Pinus* (6.8%), *Picea*+*Abies* (a total of 5.8%), *Ulmus* (5.0%), and *Betula* (4.7%) made up most of the woody pollen. A small amount of *Nitraria* and *Ephedra* (2.3%) made up the rest of the woody component. The remarkable feature was that woody plant pollen began to increase (11% to 51%), and frost-resisting conifers such as *Picea* and *Abies* appeared. At the same time, *Ulmus* and *Betula*, which are common in temperate regions, also accumulated at a certain proportion.

Strip II should be categorized as a temperate desert steppe environment with some *Betula* and *Ulmus*.

5 Discussion

The deposition of Layer 18 in the profile of SDG2 was gravel, which had a directional arrangement, indicating high-energy liquid. It should be characterized by the gravel of a riverbed. The deposition of Layer 17 was coarse to find sand, which developed inclined and interleave bedding, also indicating high-energy liquid. The transportation of deposition was mainly bound and suspension. Traction was found in the secondary position. A small amount of hydrophyte and wetland plants, along with the above-mentioned depositional characteristics reflect a river depositional environment (Table 1). The deposition of Layer 16 was grayish black silt with a block structure, in which numerous plant remnants and a small amount of gastropods were found, indicating a marsh depositional environment. The deposition of Layers 14–15 was grayish green silt, and horizontal or current bedding developed. The deposition is a combination of marginal bank and lake, indicating low-energy liquid conditions in a stable depositional environment. A small amount of hydrophyte and wetland plants grew in this area. The deposition of Layers 13–3 was still silt. However, the color of the deposition turned to hoariness or lark. The depositional environment was mainly lake. A combination of plants exhibited remarkable change based on sporopollen analysis. Wood and fern were prosperous. More temperate-zone broadleaves and conifers appeared, reflecting a gradually degenerated lake depositional environment. The ancient activities mainly presented at these layers. It implies low water level with dry lake shore when humans came here.

The depositional sequences of Shuidonggou Localities 7, 8, and 9 are similar to those of SDG2, and those of Shuidonggou Localities 1 and 12 approximate those of SDG2 (Gao et al., 2008; Liu et al., 2008). The erosion that occurred on Localities 1 and 12 at the end of the Late Pleistocene in this area resulted in the lack of upside at SDG2. The deposition of the Early and Middle Holocene accumulated after that this. Similar sequences can be found in many

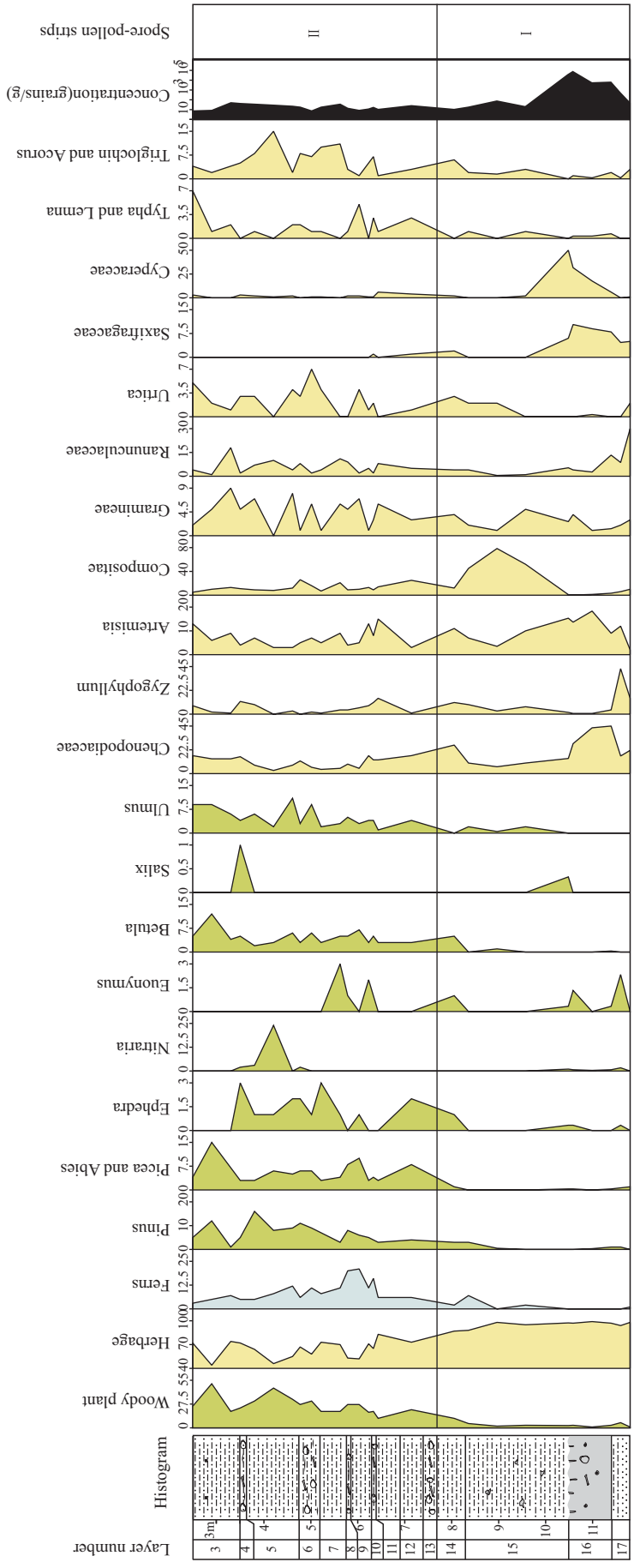

Fig. 6. Sporopollen percentage curves of SDG2.

areas at Biangou River and tributary ditches. Thus, the profile of SDG2 had representative depositional sequences in this area.

The development of the Shuidonggou ancient lake occurred at late Marine Oxygen Isotope Stage 3 (MIS 3a). Humid and warm weather during MIS3a can also be observed in China's loess and ice cores (Li and Yang, 2001; Yao, 2000). Lakes expanded visibly in western China (Li, 2000; Yang and Shi, 2003; Zheng et al., 2011). Lake sediments developed widely on the Tibetan Plateau during 40–30 ka, probably related to an increase in the seasonality of middle-to-low latitude insulation which caused an enhancement of glacier melting on the Plateau (Jiang et al., 2011). However, some researchers found that sand dune occurred at 35–25 kaBP in the Lanzhou area of the western Chinese Loess Plateau accumulation, which implies a period of increased aridity during dune formation (Long et al., 2011). The previously proposed humid MIS 3a may not be universal over all of northwest China. Our study shows that the development of Shuidonggou ancient lake has relationship to the humid climate of MIS 3a.

The sporopollen analysis of Yinchuan Basin conducted by Guobang Tong and Shuxian Fan indicated that the contents of *Picea* and *Abies* increased significantly at MIS2; this conclusion was derived on the basis of the relatively cold and dry climate (Tong et al., 1995; Fan et al., 2002). The Shuidonggou ancient lake shrank and dried out because of decreased water supplement. The evolution of rivers and lakes in the region and climate change has important links with the Late Pleistocene. Coldest whether is observed in many sites, such as the surface salinity significantly change in the northern Indian Ocean during the last glacial maximum (Mahesh, Banakar, and Burr, 2011). Liu Dongsheng, a famous Quarternary geologist, considered that there was a lake with rich aquatic species when ancient populations lived in this area (Institute of Archeology of Ningxia Hui Autonomous Region, 2003). He also pointed out that environment deteriorated because of the cold and dry wind blown in from Siberia. His viewpoint is consistent with the analysis conducted in the present work.

6 Conclusions

According to the strata, sedimentary structure, grain size, and sporopollen analysis of SDG2 profile, the depositional environment of the area generally underwent four stages at ~72–18 kaBP. During the first stage (~72–41 kaBP), a river depositional environment formed. During the second stage (41–34 kaBP), herbage flourished, reflecting warm and humid temperate grasslands with marshes. In the third stage (34–29 kaBP), herbage also flourished, indicating relatively warm and humid temperate grasslands. Plant coverage was low, and the climate turned to cool and dry during the fourth stage (29–18 kaBP). The environment is classified as a temperate desert grassland environment. It should be categorized as a degenerated lakeshore depositional environment.

Acknowledgements

This work was supported by the National Natural Science Foundation of China (Grant No. 40902013) and "Strategic Priority Research Program – Climate Change: Carbon Budget and Relevant Issues" of the Chinese Academy of Sciences (Grant No. XDA05130202). Thanks were given to Wang Huimin, Zhang Xiaoling, Zhang Yue, Ma Xiaoling, etc for their help in the field investigation and sampling during the excavation of 2004-2007.

Manuscript received July 27, 2011
accepted Apr. 16, 2012
edited by Liu Lian

References

Badanal MAHESH, Virupaxa Banakar and George Burr, 2011. Paired Measurements of Foraminiferal $d^{18}O$ and Mg/Ca Ratios of Indian Monsoons Reconstructed from Holocene to Last Glacial Record. *Acta Geologica Sinica* (English edition), 85(4): 950–956.

Fan Shuxian, Zheng Hongrui, Liu Pinggui and Guo Shengqiao, 2002. Late Quaternary sporopollen records and rapid climatic fluctuation events in the Yinxhuan basin. *Geology in China*, 29 (4): 431–434 (in Chinese with English abstract).

Gao Xing, Li Jinzeng, Madsen D.B., Brantingham P.J., Elston R. G.., and Bettinger R.L., 2002. New ^{14}C dates for Shuidonggou and related discussions. *Acta Anthropolo Sin*, 21: 211–218 (in Chinese with English abstract).

Gao Xing, Yuan Baoyin, Pei Shuwen, Wang Huimin, Chen Fuyou and Feng Xingwu, 2008. Analysis of sedimentary-geomorphologic variation and the living environment of hominids at the Shuidonggou Paleolithic site. *Chinese Sci Bull* (English edition), 53(13): 2025–2032.

Jiang, H., Mao, X., Xu, H., Thompson J., Wang, P., and Ma, X., 2011. Last glacial pollen record from Lanzhou (Northwestern China) and possible forcing mechanisms for the MIS 3 climate change in Middle to East Asia. *Quaternary Science Reviews*, 30:769–781.

Institute of Archeology of Ningxia Hui Autonomous Region, 2003. *Report of Shuidonggou site excavation in 1980*. Beijing: Science Publishing House (in Chinese), 1–233.

Li Bingyuan, 2000. The last greatest lakes on the Xizang (Tibetan) Plateau. *Acta Geographica Sinica*, 55(2): 174–181(in Chinese with English abstract).

Li Xusheng and Yang Dayuan, 2001. Magnetic susceptibility records of the Xiiashu loess since S2 and their comparisons with the marine oxygen isotope records. *Journal of Nanjing university (natural sciences)*, 37(6): 766–772(in Chinese with English abstract).

Licent E., and Teilhard de Chardin P., 1925. The Paleolithic of China. *Anthrop*, 25: 201–234 (in French)

Zhou Kunshu and Hu Jilan, 1988. Environment and stratigraphy

at the Shuidonggou site. *Acta Anthropolo Sin*, 7(3): 263–269 (in Chinese with English abstract).

Liu Decheng, Chen Fuyou, Zhang Xiaoling, Pei Shuwen, Gao Xing and Xia Zhengkai, 2008. Preliminary comments on the paleoenvironment of the Shuidonggou locality 12. *Acta Anthropolo Sin*, 27(4): 295–303 (in Chinese with English abstract).

Liu Decheng, Wang Xuelong, Gao Xing, Xia Zhengkai, Pei Shuwen, Chen Fuyou and Wang Huiming, 2009. Progress in the stratigraphy and geochronology of the Shuidonggou site, Ningxia, North China. *Chinese Sci Bull* (English edition), 54 (21): 3880–3886.

Long, H., Lai, Z., Fuchs, M., Zhang, J., and Yang, L., 2011. Palaeodunes intercalated in loess strata from the western Chinese Loess Plateau: Timing and palaeoclimatic implications, *Quaternary International*, doi:10.1016/j. quaint.2010.12.030.

Madsen, D.B., Li Jinzeng, Brantingham, P.J., Gao Xing, Elston, R.G., and Bettinger, R.L., 2001. Dating Shuidonggou and the Upper Palaeolithic blade industry in North China. *Antiquity*, 75: 706–716.

Sun Jianazhong and Zhao Jingbo, 1991. *Quaternary of Loess Plateau*. Beijing: Science Publishing House (in Chinese), 195–201.

Tong Guobang, Shi Ying, Fan Shuxian, Zhang Junpai, Song Xianhua, Liu Zhenxi, Qiao Guangdong and Zhang Jixiang, 1995. Environment features of Yinchuan basin in Late Quaternary period. *Earth Sci–J China Univer Geosci*, 20(4): 421–426 (in Chinese with English abstract).

Yang Bao and Shi Yafeng, 2003. Warm-humid climate in northwest China during the period of 40-30ka BP: Geological records and origin. *Quat Sci*, 23(1): 60–68 (in Chinese with English abstract).

Yao Tandong, 2000. Oxygen isotope stratigraphy of the Guliya ice core. *Quat Sci*, 20: 165–170 (in Chinese with English abstract).

Zheng Mianping, Liu Junying, Ma Zhibang, Wang Hailei and Ma Nina, 2011. Carbon and Oxygen Stable Isotope Values and Microfossils at 41.4–4.5 ka BP in Tai Co, Tibet, China, and Their Paleoclimatic Significance. *Acta Geologica Sinica* (English edition), 85: 1036–1056.